elsevier_BRB_8738

Research report

The tricyclic antidepressant desipramine inhibited the neurotoxic, kainate-induced $[Ca^{2+}]_i$ increases in CA1 pyramidal cells in acute hippocampal slices

István Koncz[a]

Bernadett K. Szász[b]

Szilárd I. Szabó[b]

János P. Kiss[c]

Árpád Mike[b]

Balázs Lendvai[d]

E. ~~Sylvester~~Sylvester Vizi[b]

Tibor Zelles[e, b, *]

zelles.tibor@med.semmelweis-univ.hu

zelles@koki.hu

[a]Department of Pharmacology & Pharmacotherapy, University of Szeged, Szeged, Hungary

[b]Institute of Experimental Medicine, Hungarian Academy of Sciences, Budapest, Hungary

[c]Servier, Budapest, Hungary

[d]Gedeon Richter Plc., Pharmacology and Drug Safety Department, Budapest, Hungary

[e]Department of Pharmacology and Pharmacotherapy, Semmelweis University, Budapest, Hungary

*Corresponding author~~. Dept.~~ at: Department of Pharmacology and Pharmacotherapy, Semmelweis University~~ H-1089 Budapest Nagyvárad tér 4.~~, Nagyvárad tér 4, H-1089 Budapest, Hungary. Tel.: +36 1 210 2930/56297; fax: +36 1 210 4412.

Abstract

Kainate (KA), used for modelling neurodegenerative diseases, evokes excitotoxicity. However, the precise mechanism of KA-evoked $[Ca^{2+}]_i$ increase is unexplored, especially in acute brain slice preparations. We used $[Ca^{2+}]_i$ imaging and patch clamp electrophysiology to decipher the mechanism of KA-evoked $[Ca^{2+}]_i$ rise and its inhibition by the tricyclic antidepressant desipramine (DMI) in CA1 pyramidal cells in rat hippocampal slices and in cultured hippocampal cells. The effect of KA was dose-dependent and relied totally on extracellular Ca^{2+}. The lack of effect of ~~DL~~dl-2-amino-5-phosphonopentanoic acid (AP-5) and abolishment of the response by 6-cyano-7-nitroquinoxaline-2,3-dione (CNQX) suggested the involvement of non-N-methyl-~~D~~d-aspartate receptors (non-NMDARs). The predominant role of the Ca^{2+}-impermeable α-amino-3-hydroxy-5-methyl-4-isoxazolepropionate receptors (AMPARs) in the initiation of the Ca^{2+} response was supported by the inhibitory effect of the selective AMPAR antagonist GYKI 53655 and the ineffectiveness of 1-naphthyl acetylspermine (NASPM), an inhibitor of the Ca^{2+}-permeable AMPARs. The voltage-gated Ca^{2+} channels (VGCC), blocked by ω-Conotoxin MVIIC + nifedipine + $NiCl_2$, contributed to the $[Ca^{2+}]_i$ rise. VGCCs were also involved, similarly to AMPAR current, in the KA-evoked depolarisation. Inhibition of voltage-gated Na^+ channels (VGSCs; tetrodotoxin, TTX) did not affect the depolarisation of pyramidal cells but blocked the depolarisation-evoked action potential bursts and reduced the Ca^{2+} response.

The tricyclic antidepressant DMI inhibited the KA-evoked $[Ca^{2+}]_i$ rise in a dose-dependent manner. It directly attenuated the AMPA-/KAR current, but its more potent inhibition on the Ca^{2+} response supports additional effect on VGCCs, VGSCs and Na^+/Ca^{2+} exchangers. The multitarget action on decisive players of excitotoxicity holds out more promise in clinical therapy of neurodegenerative diseases.

Keywords: Kainic acid; AMPA receptors; CA1 pyramidal cells; Rat hippocampal slices; $[Ca^{2+}]_i$; Desipramine

1 Introduction

Glutamate (Glu) mediates fast excitatory transmission in the CNS by activating its ionotropic N-methyl-Dd-aspartate (NMDA), α-amino-3-hydroxy-5-methyl-4-isoxazolepropionate (AMPA) and kainate (KA) receptors (iGluRs). AMPA receptors initiate the majority of postsynaptic depolarisation and subsequent neuronal firing in the CNS (Bredt and Nicoll, 2003). Activation of AMPA receptors also augments Ca^{2+} influx via NMDA receptors by causing depolarisation, which relieves the Mg^{2+} block. In certain neurological diseases, AMPA receptors allow cytotoxic levels of Ca^{2+} into neurons (Chang et al., 2012). Ca^{2+} plays an important role in the maintenance and control of the basic functional properties of neurones (e.g. transmitter release, gene transcription). On the other hand, an excessive elevation in intracellular calcium concentration ($[Ca^{2+}]_i$) plays a prominent role in the mediation of glutamate-induced (excitotoxic) neuronal cell death (Li et al., 2013; Sattler and Tymianski, 2001). Glutamate receptor-related excitotoxicity in neurons and oligodendrocytes, starts with the influx of Na^+ and Ca^{2+} through the stimulated receptors (McDonald et al., 1998; Sánchez-Gómez and Matute, 1999). This cation entry can trigger a secondary elevation in $[Ca^{2+}]_i$ through voltage-gated Ca^{2+} channels (VGCC). Understanding the different mechanisms of presynaptic and postsynaptic modulation of the glutamatergic transmission (Andó and Sperlágh, 2013; Iwata et al., 2013; Kobayashi et al., 2009; Liu et al., 2013) is important to identify potential drug targets able to reduce EAA receptor-related excitotoxicity.

It was reported that KA, a rigid structural analogue of glutamate, reproduces the excitotoxic action of glutamate on neurons. Due to its neurotoxic effect in the CNS, KA has long been used as a model for neurodegenerative diseases where excitotoxicity is implicated. It mimics the neurodegenerative pattern observed in Huntington's disease and causes selective damage to the hilus, CA3 and CA1 areas of the hippocampus (Coyle and Schwarcz, 1976; Coyle et al., 1983; Zheng et al., 2011) and is able to induce striatal lesions (Vécsei and Beal, 1991). KA can also be used to evoke epileptic seizures in animal models that originate in the hippocampal formation and amygdala (Ben-Ari, 1985; Nadler, 1981). AMPAR stimulation is evoked by the non-desensitising action of KA, and plays a fundamental role in ischaemic neuronal damage, as well (Cull-Candy et al., 2006; Kwak and Weiss, 2006).

The $[Ca^{2+}]_i$ rise was hypothesised to have a principal role in the mechanism of action for all of these KA-evoked disease states. Despite its widespread use, the precise mechanism of KA-evoked $[Ca^{2+}]_i$ increase is controversial, especially in acute brain slice preparations. Influx of Ca^{2+} through VGCCs, evoked by AMPAR-mediated depolarisation, is a feasible candidate. Influx of Ca^{2+} directly through the AMPAR is much less prominent than through NMDARs (Burnashev et al., 1995) and depends on the subunit composition of the receptor. Presence of the GluA2 subunit in AMPA receptors provides Ca^{2+}-impermeability to the ionotropic receptor channel, while the absence of the subunit assures the permeability of the receptor for the divalent cation. Some reports suggest that freshly isolated hippocampal pyramidal neurons lack Ca^{2+}-permeable AMPARs (Magazanik et al., 1997), while others indicate that a heterogeneous mixture of Ca^{2+}-permeable and impermeable AMPA channels were expressed on pyramidal cells in hippocampal cultures (Ogoshi and Weiss, 2003).

A growing body of evidence has indicated the involvement of glutamatergic neurotransmission in the mechanism of action of antidepressants (Martinez-Turrillas et al., 2002; Mayer et al., 2009; Szasz et al., 2007; Takebayashi et al., 2000), but the neuroprotective potential of antidepressants has also been suggested (Kiss et al., 2012).

The aim of our present work was to investigate the underlying mechanisms of Ca^{2+} entry that contribute to KA-induced increase in $[Ca^{2+}]_i$ in individual CA1 pyramidal cells of acute rat hippocampal slices and to test the effect of the antidepressant desipramine (DMI) on the KA-evoked response. While the role of Ca^{2+}-permeable AMPARs in ischaemia and other neurodegenerative diseases has been investigated extensively (Cull-Candy et al., 2006), the role of the Ca^{2+}-impermeable AMPARs in these debilitating diseases has received less attention. We found that KA activated the Ca^{2+}-impermeable AMPA receptors, causing membrane depolarisation. The subsequent opening of voltage-gated Na^+- and Ca^{2+} channels resulted in bursts of action potentials and influx of Ca^{2+} into the CA1 pyramidal cells, respectively. The VGCC-dependent Ca^{2+} influx contributed to both the depolarisation and the rise in $[Ca^{2+}]_i$ measured over the soma of the pyramidal cells. The NMDARs were not significantly involved in the Ca^{2+} response. DMI dose-dependently inhibited the AMPA/KA receptor (AMPA-/KAR) current and the KA-evoked $[Ca^{2+}]_i$ rise, suggesting a subsidiary neuroprotective property for the drug.

2 Methods

All manipulations of the animals were approved by the local committee for animal health and care and performed according to the European Communities Council Directive recommendations for the care and use of laboratory animals (86/609/CEE).

2.1 Preparation of brain slices

. Wistar rats (16-Wistar rats (16–21 days old) were anaesthetised using isoflurane and decapitated. The brain was removed and placed in ice-cold cutting solution (composition in mM: NaCl, 126; KCl, 2.5; $NaHCO_3$, 26; $CaCl_2$, 0.5; $MgCl_2$, 5; NaH_2PO_4, 1.25; and glucose, 10) which was continuously bubbled with 95% O_2 + 5% CO_2, resulting in pH 7.4. Coronal slices were cut on a vibratome (Vibratome 1000; 250 μm), separated into left and right hemispheres and transferred into a mesh-bottom holding chamber containing artificial cerebrospinal fluid (ACSF, in mM: NaCl, 126; KCl, 2.5; $NaHCO_3$, 26; $CaCl_2$, 2; $MgCl_2$, 2; NaH_2PO_4, 1.25; and glucose, 10) bubbled with a mixture of 95% O_2 + 5% CO_2, resulting in pH 7.4. After 20–25 min incubation at 35 °C, the slices were kept at room temperature for the remainder of the experiment (Zelles et al., 2001).

2.2 Intracellular calcium measurement.

The method was described previously (Fekete et al., 2009; Zelles et al., 2001). Briefly, for bulk loading of the calcium indicator, the slices were incubated in ACSF supplemented with 5 μM Fura-2/AM and 0.025% (w/v) Pluronic F-127 detergent for

50–60 min at room temperature. Subsequently, the slices were left in ACSF for at least 40 min to ensure Fura-2/AM de-esterification.

Slices were submerged and superfused with ACSF (2 ml/min) in an experimental chamber mounted on a Gibraltar BX1 platform (Burleigh) and viewed with a 40× water immersion objective (Olympus) on an Olympus BX50WI upright microscope. Drugs were put into ACSF and their administration started at least 15 min before the second KA stimulus and was maintained throughout the rest of the experiment. Field stimulation of the slices (10 Hz, 3 ms, 50 pulses) was performed using platinum electrodes placed on opposite sides of the experimental chamber. Ca^{2+}-free ACSF was prepared by substituting Ca^{2+} with 1 mM EGTA. In Ca^{2+}-free experiments, KA perfusion was started only after the Ca^{2+}-free condition had been achieved, i.e., when electrical stimulation did not produce an effect. Pyramidal cells of the CA1 region were alternately illuminated at wavelengths of 340 ± 5 nm and 380 ± 5 nm with a TILL Polychrome II monochromator. The UV illumination was attenuated by means of an adjustable diaphragm installed in the light path. The emitted light (510 ± 20 nm) was detected by a cooled CCD camera (Photometrics Quantix), and the system was controlled by Axon Imaging Workbench 2.2 software. The $[Ca^{2+}]_i$ values of cell somata were calculated off-line using the following equation:

$$[Ca^{2+}]_i = K_d \cdot \frac{F^{380}_{max}}{F^{380}_{min}} \frac{R - R_{min}}{R_{max} - R}$$

R is the ratio of emission intensity at 340 nm excitation, to emission intensity at 380 nm excitation; R_{min} is the ratio at zero free Ca^{2+}; R_{max} is the ratio at saturating Ca^{2+}; F^{380}_{max} is the fluorescence intensity at 380 nm excitation, for zero free Ca^{2+}; and F^{380}_{min} is the fluorescence intensity at saturating free Ca^{2+} (Grynkiewicz et al., 1985). Cell image intensities were background-corrected with the actual fluorescence values obtained over loaded-cell-free areas close to the investigated neuron. The parameters characterising the system, Kd, $F^{380}_{max}/F^{380}_{min}$ Fmax 380/Fmin 380, Rmin and R, R_{min} and R_{max}, were determined empirically by means of the Calcium Calibration Buffer Kit with Magnesium #2.

Neurons with resting $[Ca^{2+}]_i$ higher than 150 nM were excluded from further analysis. KA-induced $[Ca^{2+}]_i$ increases were determined by subtracting the basal level from the peak amplitude. The effect of drugs on the KA response was expressed as the ratio (Peak2/Peak 2/Peak 1) of the response in the presence (Peak2) and absence (Peak 2) and absence (Peak 1) of the drug. The data are presented as the mean ± SEM of Peak2/Peak 2/Peak 1 values obtained from individual pyramidal cells (*n values in Results and F n* values in Section 3 and figure legends). Image analysis were performed on 1–as performed on 1–5 cell somata per brain slice. Every treatment group included measurements on at least 3 different slices (3–8), prepared from at least 3 different rats (3–7). Response curves of individual neurons in certain treatment groups were averaged by Igor Pro software and the resultant traces are shown on Figs. 2 and 3 and Fig. 5A in Figs. 2, 3 and 5A and B to demonstrate the characteristics of the effect of different experimental perturbations.

2.3 Electrophysiology on slices

Patch pipettes were pulled from borosilicate glass (1.2 mm OD, Harvard Instruments). For current clamp recordings, 3–6 MΩ electrodes were filled with 125 mM K-gluconate, 20 mM KCl, 10 mM HEPES, 10 mM Di-Tris-salt phosphocreatine, 0.3 mM Na-GTP, 4 mM Mg-ATP, and 10 mM NaCl. Cells with an initial resting membrane potential more negative than– –50 mV were used. Whole-cell recordings were performed using an Axopatch 200B amplifier (Axon Instruments, Union City, CA). Data acquisition and analysis were performed using pClamp 8.1 (Axon Instruments, Union City, CA). Every treatment group included measurements on at least 3 different slices, prepared from at least 3 different rats.

2.4 Electrophysiology on cultured hippocampal cells with rapid drug application

Cell culture preparation and electrophysiology were performed as published previously (Szasz et al., 2007). Briefly, pregnant rats (17–18 day gestation) were anesthetised with the mixture of ketamine (50 mg/ml) and xylazine (10 mg/ml). Hippocampi of 4–6 foetuses were dissected out, incubated in 0.25% trypsin for 10 min, mechanically dissociated in MEM, and plated at a density of 150–300 000/35 mm poly-L-300 000/35 mm poly-L-lysine-coated Petri dishes (2 μg/ml). At 24 hour after plating, the medium was replaced with Neurobasal medium supplemented with B27. KA-evoked currents were recorded from neurons (14–21 days in vitro). Transmembrane currents were recorded by whole-cell patch clamp using an Axopatch 200B amplifier and pClamp software (Axon Instruments). All experiments were performed at room temperature. Series resistance was compensated to 60–80%. Pipettes were filled with an intracellular solution of the following composition (mM): CsCl 70, CsF 70, NaCl 10, HEPES 10, Cs-EGTA 10; pH 7.3. The composition of the external solution was (mM): NaCl 150, KCl 5, $CaCl_2$ 1.4, glucose 10, HEPES 5; tetrodotoxin 0.0003; picrotoxin 0.1; strychnine 0.002; glycine 0.01; pH 7.3. Currents were low-pass filtered at 2 kHz and sampled at 10 kHz. A pressure-operated, computer-controlled rapid drug application device (DAD-12; Adams and List) was used for drug administration. The inlets of the two glass U-tubes were connected to the pressure control unit of the DAD-12, and the outlet to a peristaltic pump, to gain precise control of both the inflow and the outflow. Drug application was evoked by closing the electric valve at the outlet of one of the U-tubes. This arrangement allowed rapid application and removal of drugs: 10–to –90% solution exchange times were in the 2–to 10 ms range.–10 ms range.

2.5 Statistical analysis

One-way ANOVA and Tukey post-hoc tests were used to determine the significance of data. Differences were considered significant at $p < 0.05$.

Materials. 2.6 Materials

The following chemicals were used: Fura-2/AM, Pluronic F-127 and Calcium Calibration Buffer Kit with Magnesium #2 (Molecular Probes, Eugene, OR, USA); DL-DL-2-amino-5-phosphonopentanoic acid (AP-5), 6-cyano-7-nitroquinoxaline-2,3-dione

disodium salt (CNQX), $CdCl_2$, EGTA, KA, nifedipine, $NiCl_2$ (Sigma Chemical Co., St. Louis, MO, USA); bicuculline, ω-conotoxin-MVIIC, GYKI 53655, 1-naphthyl acetyl spermine trihydrochloride (NASPM; Tocris, Ballwin, MO, USA); tetrodotoxin (TTX; Alomone Labs, Jerusalem, Israel); desipramine (obtained from EGIS Pharmaceutical Ltd., Budapest, Hungary). All other chemicals used were purchased from Merck (Darmstadt, Germany).

3 Results

3.1 KA evokes a repeatable, dose-dependent $[Ca^{2+}]_i$ rise in individual pyramidal cells in the CA1 region of rat hippocampal slices

To examine the relationship of KA concentrations to Ca^{2+} responses in individual CA1 pyramidal cell somata, hippocampal slices were exposed to 1, 10, 50 and 100 µM KA in the perfusion buffer for 30 sec. The KA-induced rise in $[Ca^{2+}]_i$ was dose-dependent (Fig. 1, inset). In further experiments we used 50 µM of KA. The evoked Ca^{2+} response was repeatable, and the $[Ca^{2+}]_i$ returned to baseline after termination of KA application (Fig. 1). There was an individual variability in the peak amplitudes of the KA-evoked responses between cells (329 ± 39 nM, first responses in the 16 control cells). However, in individual cells the amplitude of the second response (Peak 2) was similar to the first (Peak 1). In the control experiments, when no drug was perfused during Peak 2, the ratio of the two KA-induced Ca^{2+} elevations was near one (Peak 2/Peak 1 = 1.03 ± 0.068, ~~n = 16; Fig. 2A~~n = 16; Fig. 2A).

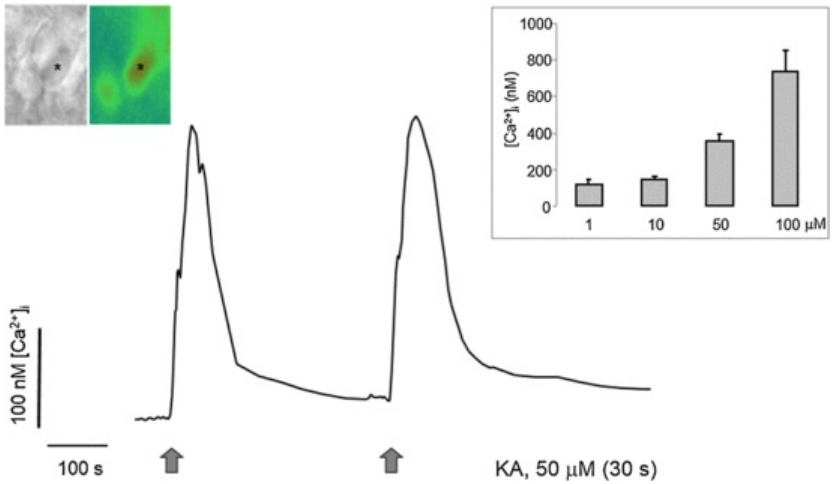

Fig~~ure~~. 1 KA evoked a dose-dependent and repeatable increase in $[Ca^{2+}]_i$ in CA1 pyramidal cells in acute rat hippocampal slices. The representative trace shows the $[Ca^{2+}]_i$ measured by fura-2 in the soma of a pyramidal neuron (see ~~Methods~~Section 2). The Ca^{2+} transients were evoked by 30 sec perfusions of 50 µM KA (the arrows show Peaks 1 and 2). The *left inset* shows the oblique illumination- and fluorescence microscopy (Ex 380 nm) images of the somata of the pyramidal neuron in which the $[Ca^{2+}]_i$ was measured (asterisk). The *right inset* illustrates the concentration-dependence of the evoked Ca^{2+} responses. Mean ± S.E.M., ~~n~~n = 7, 5, 16 and 5, respectively.

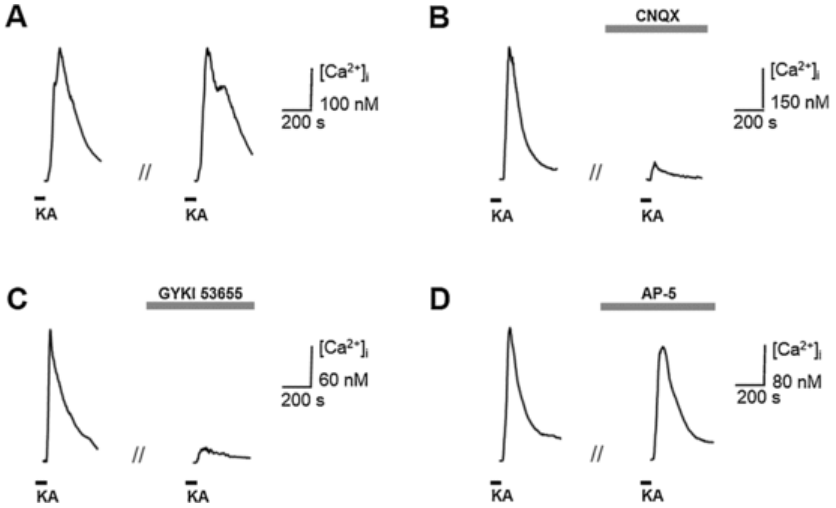

Figure. 2 Involvement of ionotropic Glu receptors in the KA-evoked $[Ca^{2+}]_i$ rise in CA1 pyramidal cells. The traces show the averages of the response curves of KA-evoked $[Ca^{2+}]_i$ rises in individual neurons in the absence (Peak 1) and presence of the indicated compounds (Peak 2). (A) Averaged Ca^{2+} transients evoked by repeated application of 50 μM KA (~~n = 16). Effects of (B~~n = 16). Effects of (B) the AMPA-/KAR antagonist CNQX (60 μM; ~~n = 7), (C~~n = 7). (C) the selective AMPA antagonist GYKI 53655 (50 μM; ~~n = 8) and (D~~n = 8) and (D) the NMDA receptor antagonist AP-5 (50 μM; ~~n~~n = 9) on the 50 μM KA-evoked $[Ca^{2+}]_i$ increase.

3.2 Characterisation of the KA-induced increases in $[Ca^{2+}]_i$

Drug effects in individual cells were normalised to the first KA-evoked response (Peak 2/Peak 1). In the presence of 60 μM CNQX, the KA-induced increase in $[Ca^{2+}]_i$ was abolished, suggesting full inhibition of AMPA/KA-Rs (Fig. 2B). The selective AMPAR antagonist GYKI 53655 (50 μM) also inhibited the KA response in the imaged cells (Fig. 2C), while the selective Ca^{2+}-permeable AMPAR inhibitor NASPM, 10 μM; Fig. 6) and the NMDAR antagonist AP-5 (50 μM; Fig. 2D) were inactive. Omission of Ca^{2+} from the perfused ACSF (+1 mM EGTA) completely negated the effect of KA (Fig. 3A). However, blockade of VGCCs by a cocktail of inhibitors (100 nM ω-Conotoxin MVIIC for N/P/Q-, 10 μM nifedipine for L- and 100 μM $NiCl_2$ for R/T-type VGCCs) only reduced the response to approximately 60% of KA-treated levels (Fig. 3B). However, the cocktail inhibited the electric field stimulation-evoked Ca^{2+} spikes, similarly to voltage-gated sodium channel (VGSCs) blockade by 1 μM TTX (data not shown). First, we tried $CdCl_2$ as a cheaper and easier way of inhibiting all of the different VGCCs, but this caused a robust, non-specific increase and plateau upon KA application (data not shown). Therefore, we did not use it in any further imaging experiments. Blocking VGSCs by TTX (1 μM) reduced the KA response to approximately 40% (Fig. 3C).

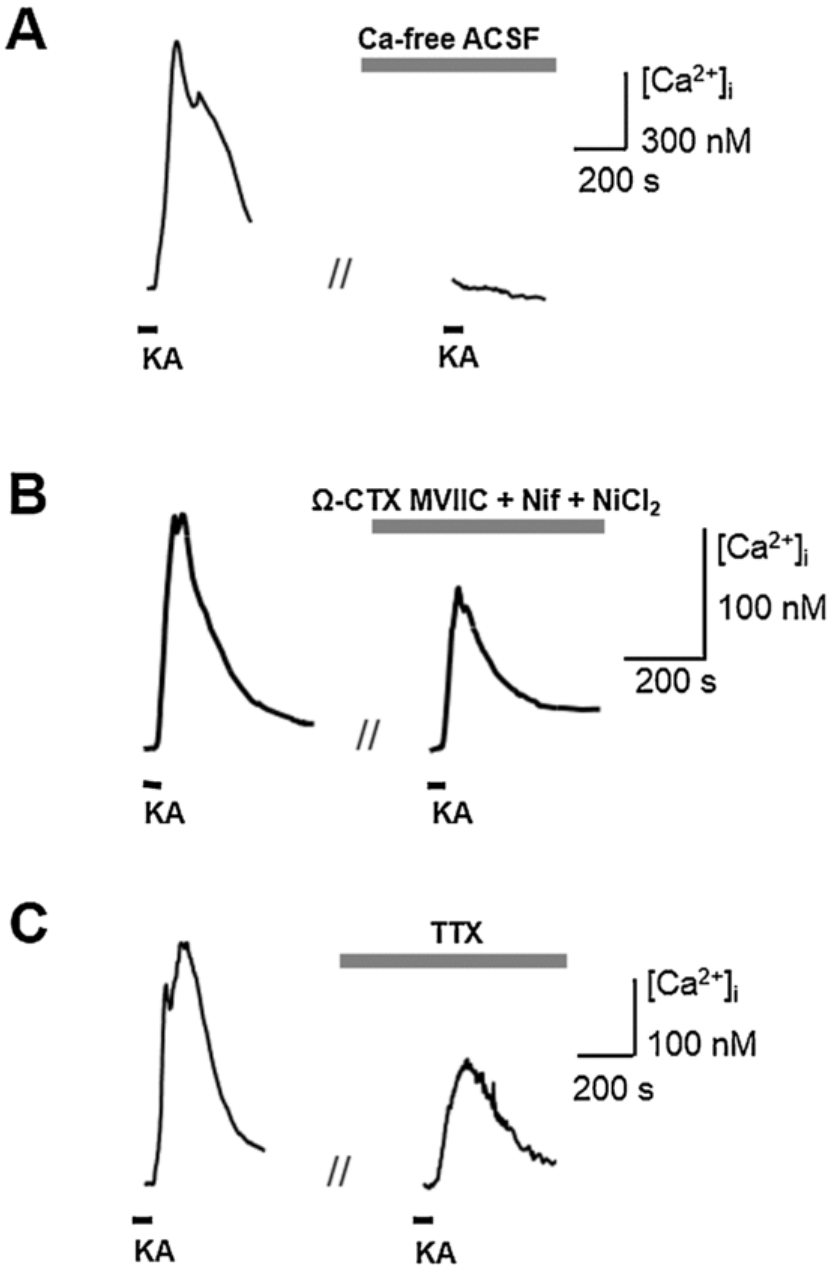

Fig~~ure.~~ 3 Role of extracellular Ca^{2+}, VGCCs and VGSCs in the KA-evoked Ca^{2+} response. The traces show the averages of the response curves of KA-evoked $[Ca^{2+}]_i$ rises in individual neurons in the absence (Peak 1) and presence of the indicated compounds (Peak 2). Effect of (~~A~~A) Ca^{2+} withdrawal (Ca^{2+}-free solution supplemented with 1 mM EGTA, ~~*n* = 6), (B~~*n* = 6), (B) the VGCC inhibitory cocktail of 100 nM ω-Conotoxin MVIIC + 20 μM nifedipine + 100 μM $NiCl_2$ (~~*n* = 6) and (C~~*n* = 6) and (C) the VGSC blocker TTX (1 μM; ~~*n*~~*n* = 9) on the 50 μM KA-evoked Ca^{2+} response.

Both Ca^{2+}- and Na^+-channels are voltage-gated; therefore, we investigated the action of KA on the membrane potential (~~*E*~~E_m) of CA1 pyramidal cells in slices. Bath perfusion of KA at 50 μM induced large membrane depolarisations (43.7 ± 3.1 mV amplitude, 52 ± 3 s~~ec~~ time to peak, 288 ± 29 s~~ec decay time, n~~ decay time, *n* = 11) in CA1 pyramidal neurons. Spontaneous firing was not observed in these slices. Action potentials were generated at the rising and the decay phases, but not at the maximal ~~*E*~~E_m

amplitude of the KA responses (Fig. 4A). TTX completely abolished firing and KA-induced increased synaptic activity (Fig. 4A). In contrast, TTX had no effect on depolarisation itself, as the depolarisation by 50 μM KA was independent of Na^+ influx via VGSCs (Fig. 4A- and B). Unlike membrane Na^+ channels, VGCCs contributed to the depolarisation by KA. In the presence of Cd^{2+} (100 μM) and Ni^{2+} (100 μM), the TTX-resistant KA response was significantly reduced by 36% (Fig. 4A- and B).

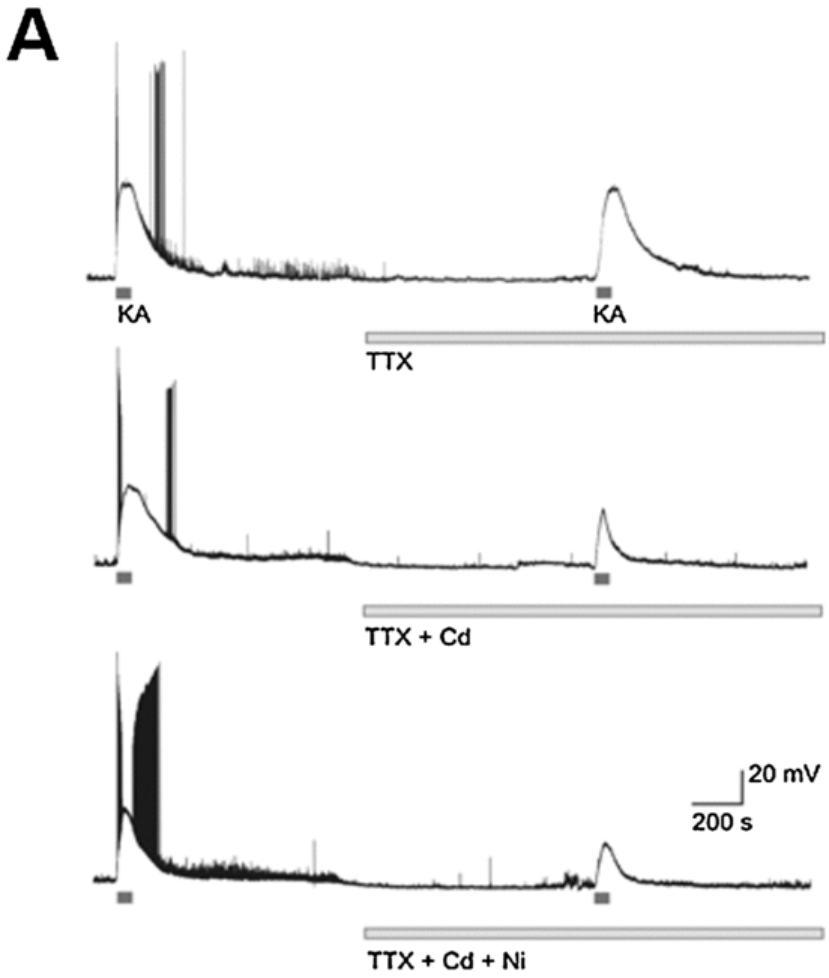

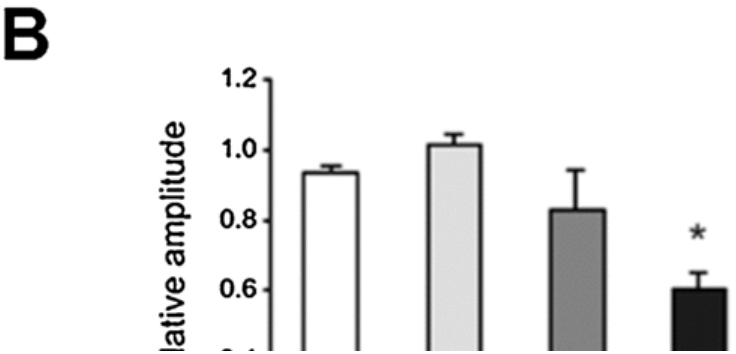

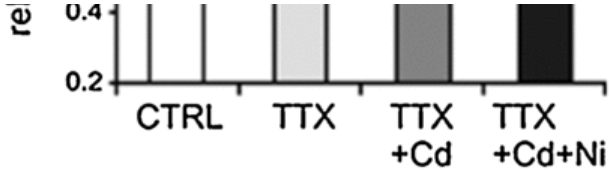

Figure. 4 Effect of KA on the membrane potential of CA1 pyramidal cells and the role of VGSCs and VGCCs in the KA-evoked response. (A) Sample traces of KA application (50 μM, 30 sec) under current clamp, indicated by the grey bar. Initial membrane resting potential was set to -70 mV. (B) –70 mV. (B) Mean depolarisation (amplitude relative to control) in control (n = 5) and in treated slices (n = 3 n = 3). TTX, tetrodotoxin 1 μM, Cd, Cd^{2+} 100 μM, Ni, Ni^{2+}, 100 μM. Drugs were administered as indicated in (A). Means ± S.E.M., * p < 0.05 Figure p ≤ 0.05.

The possible indirect effect of KA through inhibitory gamma-aminobutyric acid (GABA)-ergic neurons was tested by inhibiting the $GABA_A$ receptors. Although a slight tendency towards disinhibition appeared, 20 μM bicuculline did not significantly potentiate the KA-evoked Ca^{2+} rise. Its effect is shown in Fig. 6, which also summarises the effect of all the drugs used for deciphering the mechanism of KA action in the imaging experiments.

3.3 DMI dose-dependently inhibits the KA-induced $[Ca^{2+}]_i$ increase in individual CA1 pyramidal cells from hippocampal slices and the KA-evoked currents in cultured hippocampal cells

Superfusion of CA1 pyramidal neurons in hippocampal slices with the antidepressant drug DMI at 10, 30 and 60 μM inhibited the KA-induced $[Ca^{2+}]_i$ increase in a dose-dependent manner (Fig. 5A-B and Fig. 6s. 5A, B and 6).

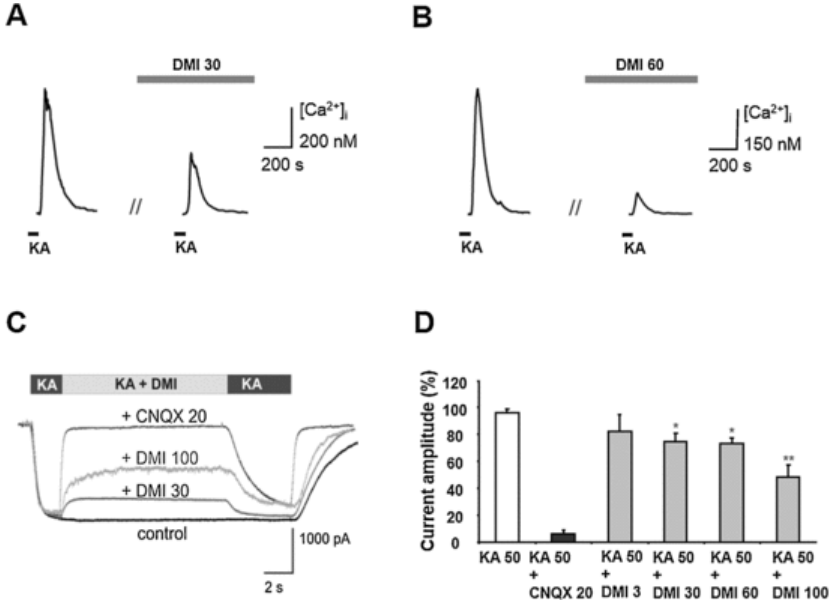

Fig. 5 DMI blocks the KA-evoked increase in $[Ca^{2+}]_i$ in CA1 pyramidal cells in slices and the AMPA-/KAR currents in cultured hippocampal cells. Effect of (A) 30 (n = 9) and (B) 60 μM (nA) 30 (n = 9) and (B) 60 μM (n = 18) DMI on the 50 μM KA-evoked Ca^{2+} response (averages of the response curves of the appropriate individual neurons). (C) Sample traces of currents evoked by KA in the absence and presence of CNQX and DMI. DMI (30 and 100 μM) was ejected from the "B" tube together with KA (50 μM) and decreased the evoked current. Application of CNQX (20 μM) abolished the current. (D) Effect of CNQX (20 μM; n = 5) and DMI (3, 30, 60, 100 μM; n = 4, 8, 10, 9, respectively) on the 50 μM KA-evoked current (n = 18 at KA 50). Data are presented as the means ± S.E.M. * p < 0.05, ** p < 0.01 Figure p ≤ 0.05, **p ≤ 0.01.

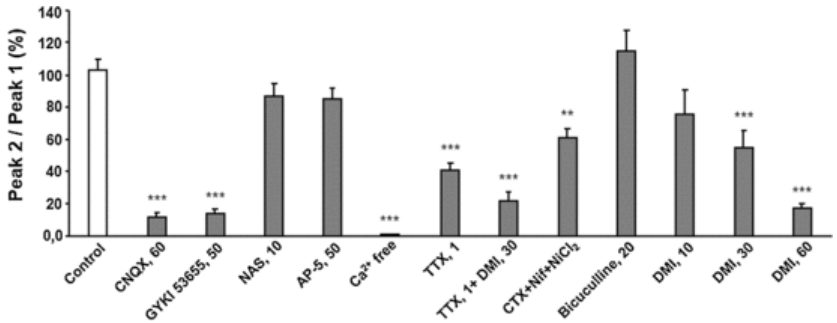

Fig. 6 Effect of different treatments on the KA-evoked $[Ca^{2+}]_i$ rise in CA1 pyramidal cells in acute rat hippocampal slices. The bar graph shows Peak 2/Peak 1 ratios as a per cent of the amplitude of KA response in the presence (Peak 2) and absence (Peak 1) of each respective compound. Data are presented as the means ± S.E.M. ~~**$p < 0.01$, ***p~~ ≤ 0.01, ***p < 0.001, compared to control. The differences between TTX 1 + DMI 30 vs. TTX 1 or DMI 30 were not statistically significant.

To investigate the effect of DMI on the AMPA/KA current directly at the receptor level, voltage clamp experiments were performed in cultured hippocampal neurons (Fig. 5C~~–~~ and D). Two glass 'U-tubes' were placed close to the patched cell for fast exchange of drugs. The "A~~–B–~~B~~–~~A" drug administration protocol was used: first 50 μM KA was administered from the "A" U tube for 2 s~~ec~~, then KA was co-applied with the tested drug for 10 s~~ec~~ from the "B" U-tube, and finally, recovery was tested by a 4 s~~ec~~ KA application ("A" U-tube). In this preparation, activation of VGCCs was excluded by keeping the membrane potential at ~~–~~70 mV. In addition, voltage-gated Na^+ and K^+ channels were blocked pharmacologically (TTX, Cs^+) during the experiment. Pressure application of 50 μM KA evoked inward currents with a relatively stable amplitude (6% decrease in amplitude). CNQX completely inhibited the KA-evoked current, which was also inhibited by DMI in a dose-dependent manner (Fig. 5C~~–~~ and D). The IC_{50} value was 131 μM.

4 Discussion

4.1 KA-evoked excitotoxicity: a model for neurodegenerative diseases

Administration of KA to rodents is used as a model for neurodegenerative diseases. Indeed, it induces seizures, glial cell activation, reactive oxygen species (ROS) production, increased release of inflammatory mediators and selective neuronal death in the hippocampus, changes that are believed to play a major role in brain isch~~a~~emia and other neurological disorders such as epilepsy or Alzheimer's disease (Wang et al., 2005; Wei et al., 2012; Zheng et al., 2011). The pathological process behind these impairments is excitotoxicity, which is the excess release of Glu and the overactivation of NMDA and non-NMDA (AMPA/KA) receptors (Cheng and Sun, 1994; Lipton, 1999; Milnerwood et al., 2010; Wang et al., 2005), synaptically or extrasynaptically (Liu and Zhao, 2013; Rodriguez et al., 2013).

KA, a non-degradable form of Glu, evokes excitotoxicity by activating AMPA-/KARs, and its use can serve as a model for elucidating the pathological mechanism of neurodegeneration. KA evokes an excessive elevation of $[Ca^{2+}]_i$ and triggers a cascade of events leading to destructive enzyme activities (proteases, lipases, nucleases), production of ROS, dysfunction of mitochondria and ultimately apoptotic and/or necrotic cell death (Fekete et al., 2009, 2008; Lipton, 1999; Wang et al., 2005).

In our experiments KA evoked an immediate, reversible and dose-dependent effect in rat hippocampal slices, providing a useful model to investigate the mechanism of action and pharmacological modulation of the KA-evoked acute $[Ca^{2+}]_i$ elevation and ~~E~~E_m changes. Its repeatability within the same experiment ensured that tests of the efficacy of specific pharmacological inhibitors were reliable for deciphering the components of the immediate KA effect.

4.2 Components of the KA-evoked effect

4.2.1 iGluRs are involved in the KA-evoked $[Ca^{2+}]_i$ increase in CA1 pyramidal cells

KA stimulates both AMPA- and KARs, but it is not an agonist for NMDARs. This finding is supported by the lack of an effect of the NMDAR antagonist AP-5 and the abolishment of the KA-evoked $[Ca^{2+}]_i$ increase by the AMPA-/KAR antagonist CNQX in the somata of CA1 pyramidal cells in our experiments. Native and recombinant KARs undergo rapid desensitisation upon agonist application. In contrast, the partial agonist KA evokes a non-decaying current on AMPA receptors. It was previously demonstrated that KA elicited only very small currents in CA1 pyramidal cells when AMPA receptors were inhibited (Jane et al., 2009). Therefore, the major component of the $[Ca^{2+}]_i$ increase in the somata of CA1 pyramidal cells in our slices was the result of AMPA receptor stimulation. This was supported by the use of the selective AMPA receptor antagonist GYKI 53655, which abolished KA-evoked elevation in $[Ca^{2+}]_i$ with a similar extent than the unselective AMPA-/KAR inhibitor CNQX. The IC_{50} of GYKI 53655 for AMPA receptors is ~1 μM, and it has no impact on KARs at concentrations up to 100 μM (Lerma et al., 2001). In addition, the KA-evoked current in cultured hippocampal neurons had no fast desensitising component. Because of the above reasons, which support that KARs have rather minor if any role in the KA-evoked $[Ca^{2+}]_i$ increase, we did not assess the potential role of KARs by selective KAR inhibitors such as NS102, UPB302, UPB296 or UPB 310 (Sun et al., 2009).

AMPARs have a tetrameric structure and the subunit composition influences their Ca^{2+} permeability. GluA2-containing receptors have low Ca^{2+} conductance, whereas AMPARs lacking the GluA2 subunit are Ca^{2+}-permeable (Burnashev et al., 1995;

Cull-Candy et al., 2006; Wang et al., 2002). Presence of the GluA2-lacking, Ca^{2+}-permeable AMPARs in hippocampal pyramidal cells is controversial. Both absence (Abushik et al., 2013) and presence (Ogoshi and Weiss, 2003) of the Ca^{2+}-permeable form of the receptor have been suggested. The lack of a significant effect of the selective Ca^{2+}-permeable AMPA receptor blocker NASPM, a synthetic analogue of joro spider toxin, in our experiments suggests the absence, or at least an inferior role for the Ca^{2+}-permeable form in the KA-evoked $[Ca^{2+}]_i$ rise. However, our result does not exclude the existence of pyramidal cells having less GluA2 relative to other subunits or a subpopulation of pyramidal cells that lack the GluA2 subunit entirely (Ogoshi and Weiss, 2003). Especially if we consider that our measurements were performed over the soma and not the dendrites, where the Ca^{2+}-permeable AMPARs are disproportionately located (Ogoshi and Weiss, 2003; Yin et al., 1999).

Although excitatory postsynaptic currents (EPSCs) in hippocampal CA1 pyramidal neurons are predominantly mediated by GluA2-containing AMPA receptors under physiological conditions (Cull-Candy et al., 2006; Wang et al., 2002), ischaemia or other neurodegenerative diseases upregulate the number of Ca^{2+}-permeable receptors, which become important contributors of the neuronal damage, especially in the postischaemic period (Cull-Candy et al., 2006; Kwak and Weiss, 2006). Upon their stimulation during excitotoxicity, GluA2-lacking AMPARs allow Ca^{2+} and Zn^{2+} influx that activates the cell death pathway (Yin et al., 2002).

Upregulation of Ca^{2+}-permeable AMPARs and their participation in the pathological rise in $[Ca^{2+}]_i$ or protection by their selective inhibition (Liu et al., 2004; Noh et al., 2005) strongly suggests a significant role for the Ca^{2+}-permeable receptor in neurological disorders, but it does not exclude the involvement of Ca^{2+}-impermeable AMPARs in the pathological process. In delayed neuronal death, there is also an immediate elevation of Ca^{2+} upon the insult, which may have a causative role in initiating and shaping the processes leading to delayed intracellular rise of the cation, and ultimately fatal damage of neurons (Hartley et al., 1993; Rego et al., 2001). Our results show that GluR2-containing, Ca^{2+}-impermeable AMPARs are suitable for inducing a cascade of events leading to significant elevation in $[Ca^{2+}]_i$. Excessive increase in $[Ca^{2+}]_i$ can initiate harmful intracellular events that are characteristic of KA- or Glu-evoked excitotoxicity.

In summary, our results suggest that KA triggered the elevation of $[Ca^{2+}]_i$ in CA1 pyramidal cells in acute slices by activating the Ca^{2+}-impermeable AMPARs, thereby causing depolarisation, which, in turn, caused activation of voltage-gated channels. Neither NMDA nor Ca^{2+}-permeable AMPARs or KARs had a significant role.

4.2.2 Mechanism of the KA-evoked depolarisation

In CA1 pyramidal neurons in acute slices, KA induced a large depolarisation in a membrane Na^+ channel independent way, as measured by TTX treatment. However, the depolarisation-evoked action potentials were prevented by TTX, indicating that the toxin was effective. Contrary to the VGSCs, blocking the VGCCs inhibited the depolarisation. Cd^{2+} is used as a non-selective VGCC blocker, but its potency is lower on T-type VGCCs (Hoehn et al., 1993). Its application together with the T/R-type VGCC blocker Ni^{2+} significantly reduced the KA-induced membrane depolarisation. Cd^{2+} alone showed a tendency towards inhibition but without statistical significance. This result indicates that, while other types of VGCCs may contribute to these responses, the T/R- type of VGCCs are certainly involved in the KA-evoked depolarisation of CA1 pyramidal cells. A relatively large part of the depolarisation was not generated by the VGCCs. Indeed, a considerable AMPA-/KAR-mediated current was measured following rapid KA administration in cultured hippocampal cells. Most likely, this current was responsible for the remaining depolarisation in the presence of voltage-gated channel blockers. Beyond their direct involvement, AMPA-/KARs also served as the trigger for VGCC activation because CNQX abolished both the KA-evoked current in cultured neurons, and the Ca^{2+} elevation in slices.

In acute slice preparations, a portion of neuronal connections are preserved, as demonstrated by the increased synaptic activity after KA administration in current clamp recordings. Activation of the excitatory input neurons by KA and the block of this synaptic activity by TTX show that KA stimulated the input neurons somatodendritically and not presynaptically, which is the predominant functional location for KARs (Jane et al., 2009). On the other hand, the lack of inhibition by TTX on the KA-induced depolarisation suggests that the KA-induced response of CA1 pyramidal neurons is dominated by direct effects of KA on the cells investigated.

We could not show a significant modulatory role for the inhibitory GABAergic inputs. Although the involvement of inhibitory neurons in KA action has been suggested (Fisher and Alger, 1984), inhibition of $GABA_A$ receptors by bicuculline did not potentiate the effect of KA on $[Ca^{2+}]_i$.

4.2.3 Molecular components involved in the KA-evoked $[Ca^{2+}]_i$ rise

Omission of Ca^{2+} from ACSF completely eliminated the KA-evoked Ca^{2+} response, indicating that Ca^{2+} influx has a substantial role in this response. Because the Ca-permeable AMPARs were not involved in the massive depolarisation induced by KA (see above), it is likely that VGCCs were involved in the response. Indeed, blockade of all types of VGCCs known to be present on the somata of CA1 pyramidal neurons (Magee and Johnston, 1995) using a cocktail of ω-conotoxin-MVIIC (N-, P-, Q-), nifedipine (L-) and $NiCl_2$ (R/T-) inhibited the KA-induced rise in $[Ca^{2+}]_i$. The VGCCs were responsible for approximately 40% of the KA-evoked Ca^{2+} signal, similar to what was found in rat retinal ganglion cells (Hartwick et al., 2008). First, we used $CdCl_2$ to block all of the VGCCs, as we did in the current clamp experiments. However, Cd^{2+} enters the cells partially through VGCCs and binds to fura-2 to increase the 340/380 ratio (Hinkle et al., 1992), which disturbed the imaging experiments. Depolarisation that activated the VGCCs could be induced by both the direct AMPAR current and the burst of action potentials, which explained TTX inhibition of the Ca^{2+} rise as well. Based on our experiments, it is not possible to determine whether the rise in $[Ca^{2+}]_i$ is exclusively the result of the influx of Ca^{2+} or also arises from other sources. The rise in $[Na^+]_i$ in in vitro models of ischaemia in acute hippocampal slices was shown to result in the reverse operation of plasma membrane or mitochondrial Na^+/Ca^{2+} exchangers (NCXs) with the consequent elevations in $[Ca^{2+}]_i$ (Fekete et al., 2009; Zhang and Lipton, 1999). In our case, the elevation in $[Na^+]_i$ could be the result of Na^+ influx through AMPARs, VGSCs or both. The statistically insignificant, but more pronounced inhibitory effect of TTX (versus VGCC channel blocker cocktail) may also support the role of NCXs that represent an additional mechanism for elevating $[Ca^{2+}]_i$ over the depolarisation-induced VGCC opening. The role of Ca^{2+}-induced Ca^{2+} release, although less probable (Fekete et al., 2009), cannot be excluded either (Nozaki et al., 1999).

4.3 Potential neuroprotective role of desipramine

The involvement of glutamatergic neurotransmission in the pathophysiology of mood disorders has been reported (Musazzi et al., 2013), as the effect of antidepressants on the Glu system, including iGluRs was also shown (Bouron and Chatton, 1999; Ishibashi et al., 2005; Martinez-Turrillas et al., 2002; Szasz et al., 2007; Takebayashi et al., 2000; Vizi et al., 2013). Chronic antidepressant treatment, but not acute, changes the expression and function of NMDA- and AMPARs (Barbon et al., 2006; Musazzi et al., 2013). The changes seems to be subunit- and region specific. Chronic DMI treatment, for example, increased the number of GluA1- and GluA2/3-containing AMPARs at synapses in the rat hippocampus, but did not change it in the frontal cortex (Martinez-Turrillas et al., 2002). Barbon et al. (2006) found a decrease of GluA3 expression both in the hippocampus and the pre-frontal/frontal cortex. Although an upregulation of AMPARs in the plasma membrane after chronic administration of DMI may appear counterintuitive from the neuroprotection point of view, but even upregulation of the target receptors in the plasma membrane after chronic administration of an otherwise effective drug is not without precedent in therapy (e.g. beta antagonist treatment preserve its cardioprotective effect despite the increased beta adrenergic receptor density (Heilbrunn et al., 1989).

Tricyclic antidepressants (TCAs) also have an acute effect on iGluRs. DMI was shown to dose-dependently antagonise the NMDA current over a concentration range of 3–100 µM (Sernagor et al., 1989). Conversely, in work performed on hippocampal cultures from mouse embryos, 50 µM DMI had no effect on 20 µM KA-evoked currents. However, in our voltage clamp experiments, DMI inhibited 50 µM KA-evoked currents. The inhibition was significant at 30 µM and reached a 50% magnitude at ~100 µM. The binding of DMI to AMPARs (Stoll and Gentile, 2005; Stoll et al., 2007) also supports the effect of DMI on AMPARs. Because the Ca^{2+}-permeable AMPARs did not play a significant role in our acute model, we could not investigate the effect of DMI on these receptors.

Activation of iGluRs results in the elevation of $[Ca^{2+}]_i$, which has a substantial role both in physiological and pathophysiological regulation in neurons. The question that arises is how antidepressants influence those mechanisms. The action of NMDA was reduced by 30 µM DMI in primary cultures of rat cortical cells (Takebayashi et al., 2000), and in primary cultures of cerebellar granule neurons, amitriptylin inhibited the NMDA effect in a dose-dependent manner, while 1 µM DMI produced some inhibition of the KA-evoked Ca^{2+} response (Cai and McCaslin, 1992). We investigated the effect of different concentrations of DMI on the KA-evoked $[Ca^{2+}]_i$ rise in an acute hippocampal slice preparation, which preserves better the original tissue structure and function. DMI inhibited the Ca^{2+} response in a dose-dependent manner more potently than the evoked current. DMI (60 µM) caused a >80% reduction in the Ca^{2+} response, comparable to the effect of 60 µM CNQX. The attenuation of the KA-induced current was only approximately 20%, which is significantly less than the total abolishment of the current by 20 µM CNQX. The difference in potency suggests the action of DMI on other components involved in the Ca^{2+} signal.

A significant fraction of the Ca^{2+} response was TTX-sensitive, suggesting that VGSCs augmented the Ca^{2+} signals. The effect of DMI on VGSCs is conceivable because inhibition of 30 µM DMI was not significantly strengthened further by TTX. Although there was a tendency towards potentiation, it is very most likely that VGSCs were at least a partially inhibited by DMI. Our previous reports confirm this possibility. We have shown that most antidepressants are potent inhibitors of neuronal sodium channels with affinities in the low micromolar concentration range (Lenkey et al., 2010). DMI is no exception; its IC_{50} value at a –60 mV holding potential was 1.68 µM (Lenkey et al., 2006).

VGCCs are also natural candidate targets of the DMI effect because depolarisation of CA1 pyramidal cells was an essential component of the KA response. Inhibition of VGCCs by TCAs, including DMI, was previously shown in synaptosomes by measuring KCl depolarisation-induced $45Ca^{2+}$ uptake (Beauchamp et al., 1995; Lavoie et al., 1990), in neuronal cultures by measuring Ca^{2+} current using voltage clamp (Choi et al., 1992; Ogata et al., 1989) and in guinea pig hippocampal slices by testing field potential changes in a low Mg^{2+}-model of epilepsy (Langosch et al., 1998). VGCCs may also be involved in the TCA effect on the excitatory amino acid-induced elevation of $[Ca^{2+}]_i$ in primary cultures of cerebellar granule cells (Cai and McCaslin, 1992). However, the inhibitory action of TCAs on the KA-evoked $[Ca^{2+}]_i$ rise in brain slice preparation has not been shown.

TCAs, including DMI, were also shown to inhibit the Na^+/Ca^{2+} exchanger (NCX; Lavoie et al., 1990). However, the inhibitory effect of DMI on the Na^+ influx, either by blocking VGSCs or antagonising AMPARs, could also attenuate the reverse operation of NCX and thus indirectly inhibit the KA-evoked $[Ca^{2+}]_i$ rise.iGluRs, VGSCs, VGCCs, NCX are all decisive players in excitotoxicity, a major determinant of cell death in both chronic neurodegenerative diseases and acute insults, like ischaemic or traumatic CNS damages. Among other mechanisms, they can initiate an excessive rise in $[Ca^{2+}]_i$ that activates different molecular effectors, leading to fatal functional and structural changes in the cells (Lipton, 1999). Theoretically, DMI and other antidepressants capable of inhibiting these pathways might possess anti-neurodegenerative and anti-ischaemic effects. The process leading to neurodegenerative cell death is not a simple linear cascade of events, but rather a complex network of interconnected pathways. Therefore, pharmacologic inhibition of a single target molecule may be easily bypassed, causing therapeutic ineffectiveness. Using multi-target drugs may hold more promise (Degracia, 2010), both against the acute insults and in the chronic neurodegenerative diseases (Danysz and Parsons, 2002).

Several psychotropics, including antidepressants, have been considered as agents exhibiting neuroprotective potential in neurodegenerative diseases (Lauterbach, 2013). Antidepressants, including DMI, has also been shown to prevent apoptosis by inhibiting the Glu-induced mitochondrial permeability transition pore opening (Tang et al., 2005). Furthermore, antiepileptic drugs with demonstrated antidepressant efficacy (valproate and lamotrigine), have provided neuroprotective effects against Glu excitotoxicity, as well (Leng et al., 2013; Zádori et al., 2009). These results all emphasize the neuroprotective potential of antidepressants.

In contrast to several other compounds, DMI has been approved for human clinical use and does not disrupt the main excitatory neurotransmission in mammals like other more selective compounds. Plasma concentrations of most antidepressants, including DMI, is are from sub-micromolar (Lenkey et al., 2010) to micromolar (Besret et al., 1996; Hennings et al., 1999), but they have been reported to accumulate in the brain with mean tissue to blood concentration ratio of approximately 10 to 1 (Argenti and D'Mello, 1994). Taking also into account that a highly structurally similar TCA drug, imipramine, has a robust (150-fold) neuron-specific accumulation (Novelli et al., 1987), DMI may reach a concentration in the brain, which can exert the above mentioned actions,

especially if we consider the individual variations in metabolism and efflux of antidepressants by the multidrug resistance transporter P-glycoprotein at the blood–brain barrier (O'Brien et al., 2012).

In our experiments, we used a brain slice preparation, which preserves several components of the functional and structural complexity of the brain and, compared to neuronal cultures or neuroblastoma cell lines, is a better tool to investigate the effects and the final outcomes of multi-target drug applications.

Conflict of interest statement

The authors declare that there are no conflicts of interest.

Acknowledgements

This work was supported by the Hungarian-French Collaborative R&I Programme on Biotechnologies (TÉT_10-1-2011-0421) and the (TÉT_10-1-2011-0421) and the Hungarian Medical Research Foundation (03-403/2009 (03-403/2009).

References

Abushik P.A., Sibarov D.A., Eaton M.J., Skatchkov S.N. and Antonov S.M., Kainate-induced calcium overload of cortical neurons in vitro: Ddependence on expression of AMPAR GluA2-subunit and down-regulation by subnanomolar ouabain, *Cell Calcium* **54**, 2013, 95–104.

Andó R.D. and Sperlágh B., The role of glutamate release mediated by extrasynaptic P2X7 receptors in animal models of neuropathic pain, *Brain Res. Bull.* **93**, 2013, 80–85.

Argenti D. and D'Mello A.P., The pharmacodynamics of desipramine and desmethyldesipramine in rats, *J. Pharmacol. Exp. Ther.* **270**, 1994, 512–519.

Barbon A., Popoli M., La Via L., Moraschi S., Vallini I., Tardito D., Tiraboschi E., Musazzi L., Giambelli R., Gennarelli M., Racagni G. and Barlati S., Regulation of editing and expression of glutamate alpha-amino-propionic-acid (AMPA)/kainate receptors by antidepressant drugs, *Biol. Psychiatry* **59**, 2006, 713–720.

Beauchamp G., Lavoie P.A. and Elie R., Differential effect of desipramine and 2-hydroxydesipramine on depolarization-induced calcium uptake in synaptosomes from rat limbic sites, *Can. J. Physiol. Pharmacol.* **73**, 1995, 619–623.

Ben-Ari Y., Limbic seizure and brain damage produced by kainic acid: mechanisms and relevance to human temporal lobe epilepsy, *Neuroscience* **14**, 1985, 375–403.

Besret L., Debruyne D., Rioux P., Bonvalot T., Moulin M., Zarifian E. and Baron J.C., A comprehensive investigation of plasma and brain regional pharmacokinetics of imipramine and its metabolites during and after chronic administration in the rat, *J. Pharm. Sci.* **85**, 1996, 291–295.

Bouron A. and Chatton J.Y., Acute application of the tricyclic antidepressant desipramine presynaptically stimulates the exocytosis of glutamate in the hippocampus, *Neuroscience* **90**, 1999, 729–736.

Bredt D.S. and Nicoll R.A., AMPA receptor trafficking at excitatory synapses, *Neuron* **40**, 2003, 361–379.

Burnashev N., Zhou Z., Neher E. and Sakmann B., Fractional calcium currents through recombinant GluR channels of the NMDA, AMPA and kainate receptor subtypes, *J. Physiol.* **485** (Pt 2), 1995, 403–418.

Cai Z. and McCaslin P.P., Amitriptyline, desipramine, cyproheptadine and carbamazepine, in concentrations used therapeutically, reduce kainate- and N-methyl-Dd-aspartate-induced intracellular Ca^{2+} levels in neuronal culture, *Eur. J. Pharmacol.* **219**, 1992, 53–57.

Chang P.K.-Y., Verbich D. and McKinney R.A., AMPA receptors as drug targets in neurological disease– – advantages, caveats, and future outlook, *Eur. J. Neurosci.* **35**, 2012, 1908–1916.

Cheng Y. and Sun A.Y., Oxidative mechanisms involved in kainate-induced cytotoxicity in cortical neurons, *Neurochem. Res.* **19**, 1994, 1557–1564.

Choi J.J., Huang G.J., Shafik E., Wu W.H. and McArdle J.J., Imipramine's selective suppression of an L-type calcium channel in neurons of murine dorsal root ganglia involves G proteins, *J. Pharmacol. Exp. Ther.* **263**, 1992, 49–53.

Coyle J.T., Ferkany J.W. and Zaczek R., Kainic acid: insights from a neurotoxin into the pathophysiology of Huntington's disease, *Neurobehav. Toxicol. Teratol.* **5**, 1983, 617–624.

Coyle J.T. and Schwarcz R., Lesion of striatal neurones with kainic acid provides a model for Huntington's chorea, *Nature* **263**, 1976, 244–246.

Cull-Candy S., Kelly L. and Farrant M., Regulation of Ca^{2+}-permeable AMPA receptors: synaptic plasticity and beyond, *Curr. Opin. Neurobiol.* **16**, 2006, 288–297.

Danysz W. and Parsons C.G., Neuroprotective potential of ionotropic glutamate receptor antagonists, *Neurotox. Res.* **4**, 2002, 119–126.

Degracia D.J., Towards a dynamical network view of brain ischemia and reperfusion. Part III: tTherapeutic implications, *J. Exp. Stroke Transl. Med.* **3**, 2010, 90–103.

Fekete A., Franklin L., Ikemoto T., Rózsa B., Lendvai B., Sylvester Vizi E. and Zelles T., Mechanism of the persistent sodium current activator veratridine-evoked Ca elevation: implication for epilepsy, *J. Neurochem.* **111**, 2009, 745–756.

Fekete A., Vizi E.S., Kovács K.J., Lendvai B. and Zelles T., Layer-specific differences in reactive oxygen species levels after oxygen-glucose deprivation in acute hippocampal slices, *Free Radic. Biol. Med.* **44**, 2008, 1010–1022.

Fisher R.S. and Alger B.E., Electrophysiological mechanisms of kainic acid-induced epileptiform activity in the rat hippocampal slice, *J. Neurosci.* **4**, 1984, 1312–1323.

Grynkiewicz G., Poenie M. and Tsien R.Y., A new generation of Ca^{2+} indicators with greatly improved fluorescence properties, *J. Biol. Chem.* **260**, 1985, 3440–3450.

Hartley D.M., Kurth M.C., Bjerkness L., Weiss J.H. and Choi D.W., Glutamate receptor-induced $^{45}Ca^{2+}$ accumulation in cortical cell culture correlates with subsequent neuronal degeneration, *J. Neurosci.* **13**, 1993, 1993–2000.

Hartwick A.T.E., Hamilton C.M. and Baldridge W.H., Glutamatergic calcium dynamics and deregulation of rat retinal ganglion cells, *J. Physiol.* **586**, 2008, 3425–3446.

Heilbrunn S.M., Shah P., Bristow M.R., Valantine H.A., Ginsburg R. and Fowler M.B., Increased beta-receptor density and improved hemodynamic response to catecholamine stimulation during long-term metoprolol therapy in heart failure from dilated cardiomyopathy, *Circulation* **79**, 1989, 483–490.

Hennings E.C., Kiss J.P., De Oliveira K., Toth P.T. and Vizi E.S., Nicotinic acetylcholine receptor antagonistic activity of monoamine uptake blockers in rat hippocampal slices, *J. Neurochem.* **73**, 1999, 1043–1050.

Hinkle P.M., Shanshala E.D. and Nelson E.J., Measurement of intracellular cadmium with fluorescent dyes. Further evidence for the role of calcium channels in cadmium uptake, *J. Biol. Chem.* **267**, 1992, 25553–25559.

Hoehn K., Watson T.W. and MacVicar B.A., Multiple types of calcium channels in acutely isolated rat neostriatal neurons, *J. Neurosci.* **13**, 1993, 1244–1257.

Ishibashi H., Eto K., Kajiwara M. and Noda M., Facilitation of spontaneous glutamate release by antidepressant drugs in rat locus coeruleus, *Neurosci. Lett.* **374**, 2005, 152–156.

Iwata S., Wakita M., Shin M.-C., Fukuda A. and Akaike N., Modulation of allopregnanolone on excitatory transmitters release from single glutamatergic terminal, *Brain Res. Bull.* **93**, 2013, 39–46.

Jane D.E., Lodge D. and Collingridge G.L., Kainate receptors: pharmacology, function and therapeutic potential, *Neuropharmacology* **56**, 2009, 90–113.

Kiss J.P., Szasz B.K., Fodor L., Mike A., Lenkey N., Kurkó D., Nagy J. and Vizi E.S., GluN2B-containing NMDA receptors as possible targets for the neuroprotective and antidepressant effects of fluoxetine, *Neurochem. Int.* **60**, 2012, 170–176.

Kobayashi M., Kojima M., Koyanagi Y., Adachi K., Imamura K. and Koshikawa N., Presynaptic and postsynaptic modulation of glutamatergic synaptic transmission by activation of alpha(1)- and beta-adrenoceptors in layer V pyramidal neurons of rat cerebral cortex, *Synapse* **63**, 2009, 269–281.

Kwak S. and Weiss J.H., Calcium-permeable AMPA channels in neurodegenerative disease and ischemia, *Curr. Opin. Neurobiol.* **16**, 2006, 281–287.

Langosch J.M., Repp M., Berger M. and Walden J., Effects of the atypical antidepressant trimipramine on field potentials in the low Mg^{2+} model in guinea pig hippocampal slices, *Eur. Neuropsychopharmacol.* **8**, 1998, 209–212.

Lauterbach E.C., Neuroprotective effects of psychotropic drugs in Huntington's disease, *Int. J. Mol. Sci.* **14**, 2013, 22558–22603.

Lavoie P.A., Beauchamp G. and Elie R., Tricyclic antidepressants inhibit voltage-dependent calcium channels and Na(+)-Ca^{2+} exchange in rat brain cortex synaptosomes, *Can. J. Physiol. Pharmacol.* **68**, 1990, 1414–1418.

Leng Y., Fessler E.B. and Chuang D.-M., Neuroprotective effects of the mood stabilizer lamotrigine against glutamate excitotoxicity: roles of chromatin remodelling and Bcl-2 induction, *Int. J. Neuropsychopharmacol.* **16**, 2013, 607–620.

Lenkey N., Karoly R., Kiss J.P., Szasz B.K., Vizi E.S. and Mike A., The mechanism of activity-dependent sodium channel inhibition by the antidepressants fluoxetine and desipramine, *Mol. Pharmacol.* **70**, 2006, 2052–2063.

Lenkey N., Karoly R., Lukacs P., Vizi E.S., Sunesen M., Fodor L. and Mike A., Classification of drugs based on properties of sodium channel inhibition: a comparative automated patch-clamp study, *PLoS Cne NE* **5**, 2010, e15568.

Lerma J., Paternain A.V., Rodríguez-Moreno A. and López-García J.C., Molecular physiology of kainate receptors, *Physiol. Rev.* **81**, 2001, 971–998.

Li H., Dong H., Li J., Liu H., Liu Z. and Li Z., Neuroprotective effect of insulin-like growth factor-1: effects on tyrosine kinase receptor (Trk) expression in dorsal root ganglion neurons with glutamate-induced excitotoxicity in vitro, *Brain Res. Bull.* **97**, 2013, 86–95.

Lipton P., Ischemic cell death in brain neurons, *Physiol. Rev.* **79**, 1999, 1431–1568.

Liu D., Yang Q. and Li S., Activation of extrasynaptic NMDA receptors induces LTD in rat hippocampal CA1 neurons, *Brain Res. Bull.* **93**, 2013, 10–16.

Liu S., Lau L., Wei J., Zhu D., Zou S., Sun H.-S., Fu Y., Liu F. and Lu Y., Expression of Ca(2+)-permeable AMPA receptor channels primes cell death in transient forebrain ischemia, *Neuron* **43**, 2004, 43–55.

Liu S. and Zhao M., Neuroprotective effect of estrogen: role of nonsynaptic NR2B-containing NMDA receptors, *Brain Res. Bull.* **93**, 2013, 27–31.

Magazanik L.G., Buldakova S.L., Samoilova M.V., Gmiro V.E., Mellor I.R. and Usherwood P.N., Block of open channels of recombinant AMPA receptors and native AMPA/kainate receptors by adamantane derivatives, *J. Physiol.* **505** (Pt 3), 1997, 655–663.

Magee J.C. and Johnston D., Characterization of single voltage-gated Na^{+} and Ca^{2+} and Ca^{2+} channels in apical dendrites of rat CA1 pyramidal neurons, *J. Physiol.* **487** (Pt 1), 1995, 67–90.

Martinez-Turrillas R., Frechilla D. and Del Río J., Chronic antidepressant treatment increases the membrane expression of AMPA receptors in rat hippocampus, *Neuropharmacology* **43**, 2002, 1230–1237.

Mayer A., Szasz B.K. and Kiss J.P., Inhibitory effect of antidepressants on the NMDA-evoked [(3)H]noradrenaline release from rat hippocampal slices, *Neurochem. Int.* **55**, 2009, 383–388.

McDonald J.W., Althomsons S.P., Hyrc K.L., Choi D.W. and Goldberg M.P., Oligodendrocytes from forebrain are highly vulnerable to AMPA/kainate receptor-mediated excitotoxicity, *Nat. Med.* **4**, 1998, 291–297.

Milnerwood A.J., Gladding C.M., Pouladi M.A., Kaufman A.M., Hines R.M., Boyd J.D., Ko R.W.Y., Vasuta O.C., Graham R.K., Hayden M.R., Murphy T.H. and Raymond L.A., Early increase in extrasynaptic NMDA receptor signaling and expression contributes to phenotype onset in Huntington's disease mice, *Neuron* **65**, 2010, 178–190.

Musazzi L., Treccani G., Mallei A. and Popoli M., The action of antidepressants on the glutamate system: regulation of glutamate release and glutamate receptors, *Biol. Psychiatry* **73**, 2013, 1180–1188.

Nadler J.V., Minireview. Kainic acid as a tool for the study of temporal lobe epilepsy, *Life Sci.* **29**, 1981, 2031–2042.

Noh K.-M., Yokota H., Mashiko T., Castillo P.E., Zukin R.S. and Bennett M.V.L., Blockade of calcium-permeable AMPA receptors protects hippocampal neurons against global ischemia-induced death, *Proc. Natl. Acad. Sci. U. S. A.* **102**, 2005, 12230–12235.

Novelli A., Lysko P.G. and Henneberry R.C., Uptake of imipramine in neurons cultured from rat cerebellum, *Brain Res.* **411**, 1987, 291–297.

Nozaki H., Tanaka K., Gomi S., Mihara B., Nogawa S., Nagata E., Kondo T. and Fukuuchi Y., Role of the ryanodine receptor in ischemic brain damage—localized reduction of ryanodine receptor binding during ischemia in hippocampus CA1, *Cell. Mol. Neurobiol.* **19**, 1999, 119–131.

O'Brien F.E., Clarke G., Fitzgerald P., Dinan T.G., Griffin B.T. and Cryan J.F., Inhibition of P-glycoprotein enhances transport of imipramine across the blood–brain barrier: microdialysis studies in conscious freely moving rats, *Br. J. Pharmacol.* **166**, 2012, 1333–1343.

Ogata N., Yoshii M. and Narahashi T., Psychotropic drugs block voltage-gated ion channels in neuroblastoma cells, *Brain Res.* **476**, 1989, 140–144.

Ogoshi F. and Weiss J.H., Heterogeneity of Ca^{2+} Ca^{2+} permeable AMPA/kainate channel expression in hippocampal pyramidal neurons: fluorescence imaging and immunocytochemical assessment, *J. Neurosci.* **23**, 2003, 10521–10530.

Rego A.C., Ward M.W. and Nicholls D.G., Mitochondria control ampa/kainate receptor-induced cytoplasmic calcium deregulation in rat cerebellar granule cells, *J. Neurosci.* **21**, 2001, 1893–1901.

Rodriguez M., Sabate M., Rodriguez-Sabate C. and Morales I., The role of non-synaptic extracellular glutamate, *Brain Res. Bull.* **93**, 2013, 17–26.

Sánchez-Gómez M.V. and Matute C., AMPA and kainate receptors each mediate excitotoxicity in oligodendroglial cultures, *Neurobiol. Dis.* **6**, 1999, 475–485.

Sattler R. and Tymianski M., Molecular mechanisms of glutamate receptor-mediated excitotoxic neuronal cell death, *Mol. Neurobiol.* **24**, 2001, 107–129.

Sernagor E., Kuhn D., Vyklicky L. and Mayer M.L., Open channel block of NMDA receptor responses evoked by tricyclic antidepressants, *Neuron* **2**, 1989, 1221–1227.

Stoll L. and Gentile L., Linking tricyclic antidepressants to ionotropic glutamate receptors, *Biochem. Biophys. Res. Commun.* **333**, 2005, 622–627.

Stoll L., Seguin S. and Gentile L., Tricyclic antidepressants, but not the selective serotonin reuptake inhibitor fluoxetine, bind to the S1S2 domain of AMPA receptors, *Arch. Biochem. Biophys.* **458**, 2007, 213–219.

Sun H.Y., Bartley A.F. and Dobrunz L.E., Calcium-permeable presynaptic kainate receptors involved in excitatory short-term facilitation onto somatostatin interneurons during natural stimulus patterns, *J. Neurophysiol.* **101**, 2009, 1043–1055.

Szasz B.K., Mike A., Karoly R., Gerevich Z., Illes P., Vizi E.S. and Kiss J.P., Direct inhibitory effect of fluoxetine on N-methyl-Dd-aspartate receptors in the central nervous system, *Biol. Psychiatry* **62**, 2007, 1303–1309.

Takebayashi M., Kagaya A., Inagaki M., Kozuru T., Jitsuiki H., Kurata K., Okamoto Y. and Yamawaki S., Effects of antidepressants on gamma-aminobutyric acid- and N-methyl-Dd-aspartate-induced intracellular Ca(2+) concentration increases in primary cultured rat cortical neurons, *Neuropsychobiology* **42**, 2000, 120–126.

Tang T.-S., Slow E., Lupu V., Stavrovskaya I.G., Sugimori M., Llinás R., Kristal B.S., Hayden M.R. and Bezprozvanny I., Disturbed Ca^{2+} signaling and apoptosis of medium spiny neurons in Huntington's disease, *Proc. Natl. Acad. Sci. U. S. A.* **102**, 2005, 2602–2607.

Vécsei L. and Beal M.F., Comparative behavioral and neurochemical studies with striatal kainic acid- or quinolinic acid-lesioned rats, *Pharmacol. Biochem. Behav.* **39**, 1991, 473–478.

Vizi E.S., Kisfali M. and Lőrincz T., Role of nonsynaptic GluN2B-containing NMDA receptors in excitotoxicity: evidence that fluoxetine selectively inhibits these receptors and may have neuroprotective effects, *Brain Res. Bull.* **93**, 2013, 32–38.

Wang Q., Yu S., Simonyi A., Sun G.Y. and Sun A.Y., Kainic acid-mediated excitotoxicity as a model for neurodegeneration, *Mol. Neurobiol.* **31**, 2005, 3–16.

Wang S., Jia Z., Roder J. and Murphy T.H., AMPA receptor-mediated miniature synaptic calcium transients in GluR2 null mice, *J. Neurophysiol.* **88**, 2002, 29–40.

Wei X.-W., Yan H., Xu B., Wu Y.-P., Li C. and Zhang G.-Y., Neuroprotection of co-activation of GABA receptors by preventing caspase-3 denitrosylation in KA-induced seizures, *Brain Res. Bull.* **88**, 2012, 617–623.

Yin H.Z., Sensi S.L., Carriedo S.G. and Weiss J.H., Dendritic localization of Ca(2+)-permeable AMPA/kainate channels in hippocampal pyramidal neurons, *J. Comp. Neurol.* **409**, 1999, 250–260.

Yin H.Z., Sensi S.L., Ogoshi F. and Weiss J.H., Blockade of Ca^{2+}-permeable AMPA/kainate channels decreases oxygen-glucose deprivation-induced Zn^{2+} accumulation and neuronal loss in hippocampal pyramidal neurons, *J. Neurosci.* **22**, 2002, 1273–1279.

Zádori D., Geisz A., Vámos E., Vécsei L. and Klivényi P., Valproate ameliorates the survival and the motor performance in a transgenic mouse model of Huntington's disease, *Pharmacol. Biochem. Behav.* **94**, 2009, 148–153.

Zelles T., Franklin L., Koncz I., Lendvai B. and Zsilla G., The nootropic drug vinpocetine inhibits veratridine-induced $[Ca^{2+}]_i$ increase in rat hippocampal CA1 pyramidal cells, *Neurochem. Res.* **26**, 2001, 1095–1100.

Zhang Y. and Lipton P., Cytosolic Ca^{2+} changes during in vitro ischemia in rat hippocampal slices: major roles for glutamate and Na+-dependent Ca^{2+}-dependent Ca^{2+} release from mitochondria, *J. Neurosci.* **19**, 1999, 3307–3315.

Zheng X.-Y., Zhang H.-L., Luo Q. and Zhu J., Kainic acid-induced neurodegenerative model: potentials and limitations, *J. Biomed. Biotechnol.* **2011**, 2011, 457079.

Highlights

- KA evoked $[Ca^{2+}]_i$ rise in CA1 pyramidal cell somata in rat hippocampal slices.
- Ca^{2+}-impermeable AMPA receptors, VGSCs and VGCCs were involved in the Ca^{2+} response.
- VGCCs contributed to the KA-evoked depolarisation, VGSCs did not.
- DMI dose-dependently inhibited the AMPA-/KAR current and the KA-evoked $[Ca^{2+}]_i$ rise.
- The inhibitory, multitarget action of DMI might protect against excitotoxicity.

Queries and Answers

Query: Please confirm that given names and surnames have been identified correctly.

Answer: They are correct.

elsevier_BRB_8738

Query: One or more sponsor names and the sponsor country identifier may have been edited to a standard format that enables better searching and identification of your article. Please check and correct if necessary.

Answer: This is correct.